

<https://doi.org/10.1038/s40494-025-02139-2>

# The Hellenistic - Roman transition in glass technology: insights from Nysa-Scythopolis

Check for updates

Gry H. Barfod<sup>1</sup>, Ian C. Freestone<sup>2</sup>, Ruth Jackson-Tal<sup>3</sup>, Alicia M. Cruz-Uribe<sup>4</sup>, Achim Lichtenberger<sup>5</sup>✉ & Oren Tal<sup>6</sup>

Slumped bowls from Tell Izṭabba pre-date the site's destruction in 107 BCE, allowing for investigation of Hellenistic translucent glass with a terminus ante quem. LA-ICP-MS of thirty shards reveal two groups. While IZT-2 glasses correspond to Levantine glass of the Roman period, IZT-1 glass has lower Al<sub>2</sub>O<sub>3</sub>, MgO, FeO, Ti and higher ε<sub>Hf</sub> at a given <sup>87</sup>Sr/<sup>86</sup>Sr value. Attention is drawn to the decline in Al<sub>2</sub>O<sub>3</sub> contents of known primary glass production from South to North on the Syro-Palestinian coast. Based on this, it is suggested that IZT-1 glass originated north of Beirut. Colourless glasses typically contain both manganese and antimony. It appears that antimony was added to glass already containing manganese to improve the colour. Hence the assemblage provides insights into two important technological changes that underpinned the early Roman expansion in glass production of the period – a shift in the location of production and the development of decolourisation.

Glass production underwent a marked expansion in the late 2nd century BCE, evidenced in particular by the widespread appearance of monochrome slumped (“cast”) bowls in the archaeological record of the eastern Mediterranean. As the widely used label “Syro-Palestinian bowl” suggests, these vessels are generally considered to have been produced in the Levant, where large numbers have been recovered<sup>1</sup> and, more specifically, at Tel Anafa, Israel<sup>2</sup>, as well as at Beirut, Lebanon<sup>3,4</sup>. Recent work suggests that these types of monochrome bowl first appear in Syria-Palestine in the latter part of the 2nd century BCE, possibly in the final third or quarter of the century<sup>5</sup>.

In addition to the cultural factors, which drove the increased desire of consumers for glass vessels<sup>1,6,7</sup>, their production required a substantial increase in the availability of glass material, implying a significant increase in raw glass production as some historical sources may attest (Strabo, Geography 16.2.25; Pliny, Nat. Hist. 36.190–191; Flavius Josephus, War II.188–191), which would have involved the expansion of primary glass-making centres, as well as the spread of vessel fabrication workshops. However, we have limited understanding of the structure of the glass industry before the Roman period including how, and the extent to which, production was divided between the production of raw glass and the fabrication of vessels. Furthermore, the location of production is unclear. The glass industry in Egypt is understood to have been technically sophisticated and focused on complex plaques and vessels from strongly coloured,

colourless and opaque glass, a tradition stretching back into the Late Bronze Age<sup>8–10</sup>. The interaction between the glass industries of Egypt and the Levant as well as the contribution of Egyptian glass to the corpus of vessels known from the Levant and elsewhere is also not well understood.

In the earlier first millennium BCE, additions of antimony were used to decolourise the glass by oxidising divalent iron and thus weakening the natural blue tint; a practise observed in glass from Nimrud which continued through to—or reoccurred—in the Hellenistic period<sup>11–13</sup>. In the 2nd century BCE, however, the addition of manganese oxide to weaken the colouration due to naturally occurring iron in the glassmaking sand appears to have become dominant<sup>11,14</sup>. How, when and where this technological change occurred is unclear.

The late Hellenistic expansion in the production of translucent and manganese-decoloured glass underpinned the dramatic spread of glass technology under the Romans in the first century CE. Mass-produced and manganese-decoloured glass spread across the Empire, initially in the form of slumped bowls, but then through the widespread adoption of the blowing technique, thought to have originated in the southern Levant but which spread as far as Gaul and Britain in the Northwest and into the Sasanian world to the East.

The analysis of glass from the Hellenistic period therefore has the potential to address questions of major interest about the development of glass technology and production in the eastern Mediterranean. The present

<sup>1</sup>Cobb Meadow Research, Camden, ME, USA. <sup>2</sup>Institute of Archaeology, UCL, London, UK. <sup>3</sup>Archaeology Wing, Israel Museum, Jerusalem, Israel. <sup>4</sup>School of Earth and Climate Sciences, University of Maine, Orono, ME, USA. <sup>5</sup>Institut für Klassische Archäologie und Christliche Archäologie, Universität Münster, Münster, Germany. <sup>6</sup>Department of Archaeology and Ancient Near Eastern Cultures, Tel Aviv University, Tel Aviv, Israel. ✉e-mail: [lichtenb@uni-muenster.de](mailto:lichtenb@uni-muenster.de)

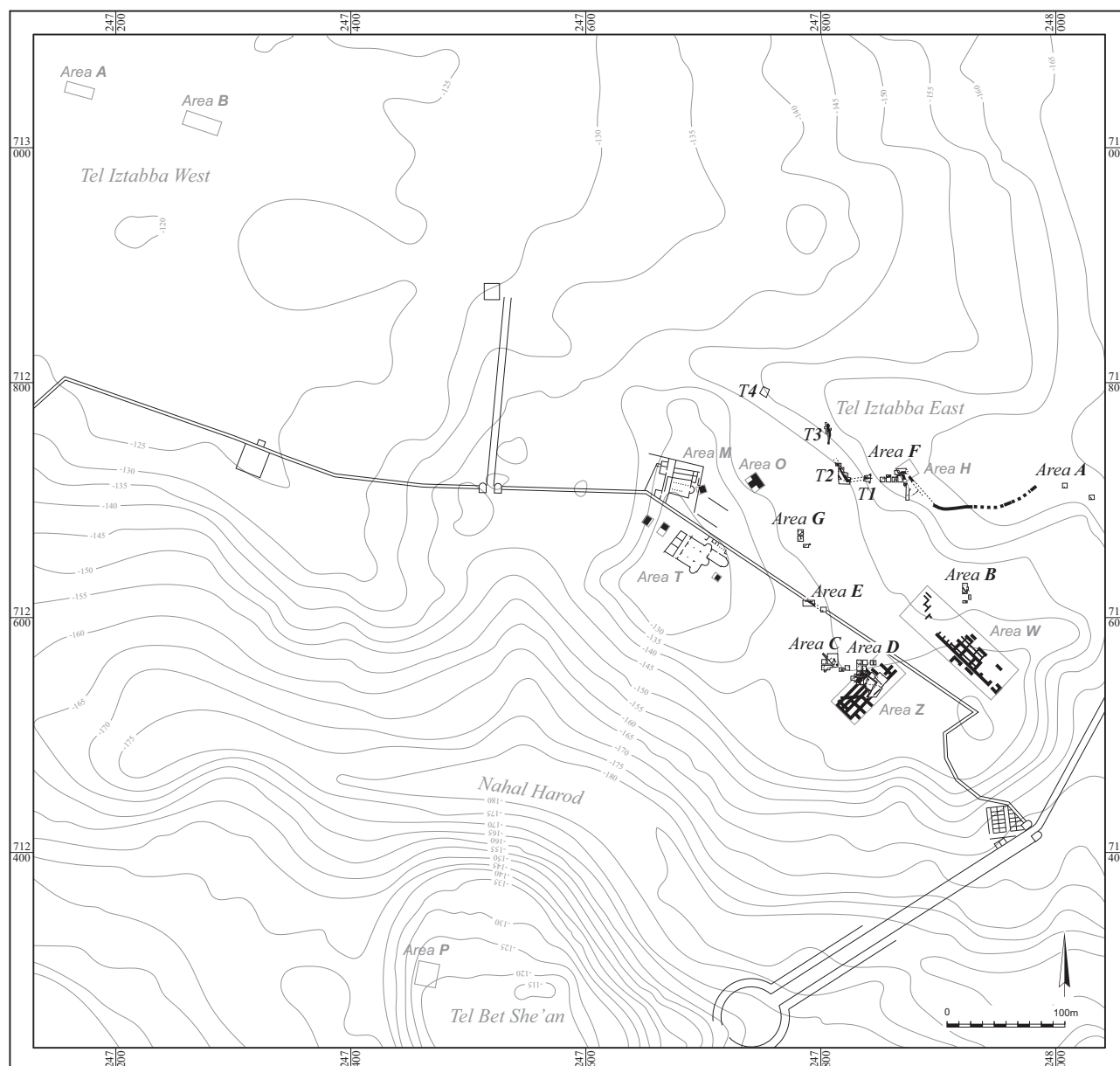


**Fig. 1** | Excavation site at Tell Izṭabba. Map excavation site at Tell Izṭabba. Source: German-Israeli Tell Izṭabba Excavation Project (GITIEP).

investigation addresses the compositions of an assemblage of bowls from Tell Izṭabba, a mound in the northern part of modern Beth Shean, Israel (Fig. 1). Tell Izṭabba, located on the northern edge of the Beth-Shean Valley in Israel, is a site with significant Hellenistic remains (Fig. 1). Situated strategically near ancient trade routes and abundant water sources, it formed part of the Seleucid founded-city of Nysa-Scythopolis under Antiochus IV in the 160 s BCE. The settlement flourished until its destruction in 107 BCE by the Hasmoneans, under John Hyrcanus<sup>15</sup>. The German-Israeli Tell Izṭabba Excavation Project (GITIEP), initiated in 2019, aims to systematically study and contextualise the site within the broader Hellenistic world. GITIEP has undertaken excavation campaigns in 2019, 2020, 2023 and 2025, and uncovered a rich and diverse range of material culture that illuminates daily life in a Seleucid urban centre<sup>16,17</sup>. Excavations have revealed domestic architecture sealed by the 107 BCE destruction layer that contained household items, ceramics, metal objects, and numerous amphorae, particularly Rhodian with stamped handles. Prominent glass finds are slumped (“cast”) monochrome bowls<sup>5,18</sup> that are the subject of the current study. The yielded slumped glass vessels can be confidently dated to the

second half of the 2nd BCE and even to the last quarter (or third) of this century. We have analysed 30 samples of late Hellenistic colourless and naturally coloured bowls (Table 1). Examples of the analysed glass are shown in Fig. 2.

## Methods

Small 1 x 1mm fresh glass shards were chipped from the vessel fragments to avoid exposed and potentially corroded surfaces, mounted in epoxy, polished, and analysed for major and trace elements by Laser Ablation Inductively Coupled Plasma Mass Spectrometry (LA-ICP-MS) at the MAGIC Laboratory at the University of Maine. Subsets were analysed for strontium (Sr) and hafnium (Hf) isotopes (nine samples) as well as for neodymium (Nd) isotopes (four samples) by Multi-Collector ICP-MS at the GeoAnalytical Lab, Washington State University.

## LA-ICP-MS

Major and trace element compositions of glasses were determined using a NWR193<sup>UC</sup> Excimer laser ablation system coupled to an Agilent 8900

**Table 1 | Summary of glass samples analysed in this study**

Sample No. #	License/Season	Locus	Basket	Type	Colour	Contextualised date
1	G-70/2019	202	2008	Cast, grooved	Colourless	Ca. 130–107 BCE
2	G-70/2019	205	2035	Cast, grooved	Greenish	Ca. 130–107 BCE
3	G-70/2019	205	2046/1	Cast, grooved	Bluish	Ca. 130–107 BCE
4	G-70/2019	205	2046/2	Cast, grooved	Yellowish	Ca. 130–107 BCE
5*	G-70/2019	209	2103/1	Cast, grooved	Amber	Ca. 130–107 BCE
6*	G-70/2019	209	2103/2	Cast, grooved	Amber	Ca. 130–107 BCE
7*	G-70/2019	209	2103/3	Cast, grooved	Colourless	Ca. 130–107 BCE
8	G-70/2019	241	2251	Cast, grooved	Amber	Ca. 130–107 BCE
9	G-70/2019	314	3091	Cast, grooved	Yellowish	Ca. 130–107 BCE
10*	G-70/2019	321	3067	Cast, grooved	Colourless	Ca. 130–107 BCE
11	G-70/2019	326	3113	Cast, grooved	Yellowish	Ca. 130–107 BCE
12	G-70/2019	337	3240	Cast, grooved	Greenish	Ca. 130–107 BCE
13*	G-17/2020	401	4022	Cast, grooved	Colourless	Ca. 130–107 BCE
14*	G-17/2020	433	4192	Cast, grooved	Colourless	Ca. 130–107 BCE
15	G-11/2023	602	6069	Cast, grooved	Yellowish	Ca. 130–107 BCE
16	G-11/2023	642	6316	Cast, grooved	Colourless	Ca. 130–107 BCE
17	G-11/2023	703	7045	Cast, grooved	Colourless	Ca. 130–107 BCE
18	G-11/2023	703	7213	Cast, grooved	Greenish	Ca. 130–107 BCE
19	G-11/2023	705	7176	Cast, grooved	Bluish	Ca. 130–107 BCE
20	G-11/2023	706	7160	Cast, grooved	Yellowish	Ca. 130–107 BCE
21	G-11/2023	707	7171	Cast, grooved	Yellowish	Ca. 130–107 BCE
22	G-11/2023	707	7205/1	Cast, grooved	Amber	Ca. 130–107 BCE
23	G-11/2023	707	7205/2	Cast, grooved	Amber	Ca. 130–107 BCE
24	G-11/2023	709	7182/1	Cast, grooved	Greenish	Ca. 130–107 BCE
25	G-11/2023	709	7182/2	Cast, grooved	Colourless	Ca. 130–107 BCE
26	G-11/2023	709	7241	Cast, grooved	Amber	Ca. 130–107 BCE
27	G-11/2023	716	7275	Cast, grooved	Colourless	Ca. 130–107 BCE
28	G-11/2023	717	7227	Cast, grooved	Greenish	Ca. 130–107 BCE
29	G-11/2023	732	7341	Cast, grooved	Yellowish	Ca. 130–107 BCE
30	G-11/2023	733	7326	Cast, grooved	Colourless	Ca. 130–107 BCE

Asterix refers to drawn typology in Fig. 2a.

ICP-MS (Supplementary Data 1–3). Analyses (four repeats on each glass) were performed using a 50 µm round spot with a beam energy density of ~3 J/cm<sup>2</sup> at a laser repetition rate of 12 Hz. Each analysis consisted of 35 s ablation followed by 18 s washout time. Approximately 20 spots on unknown samples were bracketed by two analyses each of NIST 610, NIST SRM612, GSE-1G, GSC-1G, GSD-1G, T1-G, and ATHO-G. The monitored isotopes and their dwell times can be found in Supplementary Data 3. Data reduction was done in the iolite 4 software<sup>19</sup>. Trace element contents were determined relative to USGS glass GSE-G1 using the Trace Elements 3D data reduction scheme by summing all analysed elements in the unknown glasses to 98%. Summing to 98% was done to take into account elements in the glass that were not measured by LA-ICPMS including Cl, P<sub>2</sub>O<sub>5</sub> and SO<sub>2</sub>. Major and trace element LA-ICP-MS data are reported as the mean of four repeat analyses on each glass chip (Supplementary Data 1). Results for secondary reference glasses (GSC-G1, GSD-G1, ATHO-G, NIST-SRM610, and NIST-SRM612, *n* = 10<sup>20</sup>) give an estimate of reproducibility and accuracy. The results show reproducibility better than 4% for most elements, while accuracy is within 5% for most elements (Supplementary Data 2). Most of the samples are decoloured or naturally coloured from iron in the glass making sands and generally devoid of inclusions, colourants and/or opacifiers. Thus the laser sampled base glass plus decolourants.

### MC-ICP-MS

Based on the LA-ICP-MS data set, a subset of samples was selected for Sr, Nd and Hf isotope analyses. The aim was to obtain isotope data for glass that covered the observed ranges in CaO, Al<sub>2</sub>O<sub>3</sub>/SiO<sub>2</sub>, Mn and Sb contents. 10–30 mg fresh glass was dissolved in concentrated HNO<sub>3</sub> and HF (1:10) followed by purification of strontium, neodymium and hafnium by chromatographic methods<sup>21</sup>. All reagents were distilled and shown to have low blanks corresponding to Optima grade. Mass fractionation correction of measured <sup>87</sup>Sr/<sup>86</sup>Sr ratios by Neptune MC-ICP-MS was done by adjusting the measured <sup>87</sup>Sr/<sup>86</sup>Sr ratios to the natural <sup>86</sup>Sr/<sup>88</sup>Sr ratio = 0.1194. Monitored signals below a few mV on masses 84 (<sup>84</sup>Kr + <sup>84</sup>Sr) and 85 (<sup>85</sup>Rb) showed negligible interferences of <sup>87</sup>Rb on <sup>87</sup>Sr and <sup>86</sup>Kr on <sup>86</sup>Sr. The <sup>87</sup>Sr/<sup>86</sup>Sr ratios of the samples were normalised to an accepted value of 0.710248 for the SRM 987 standard by repeated analysis of this standard for every third sample. The Corning B standard result of <sup>87</sup>Sr/<sup>86</sup>Sr of 0.709052 ± 0.000010 compares well to our previous results of 0.708989 ± 0.000013<sup>21</sup>. Hf and Nd separations were on Eichrom® Ln-spec with HCl-HF and HCl dilutions, respectively. During analysis, mass fractionation was corrected for by normalising to the known natural ratio of <sup>179</sup>Hf/<sup>177</sup>Hf of 0.732527. Analysis of Ames Hf standard JMC-475 (*n* = 15) yielded <sup>176</sup>Hf/<sup>177</sup>Hf ratio of 0.282165 ± 0.000015 (2δ), while USGS basalt standards BHVO-2 (*n* = 9) and BCR-2 (*n* = 3) yielded 0.283104 ± 0.000010 (2δ) (compared to Georem value = 0.283104 ± 0.000010) and 0.282878 ± 0.000013 (2δ) (compared to

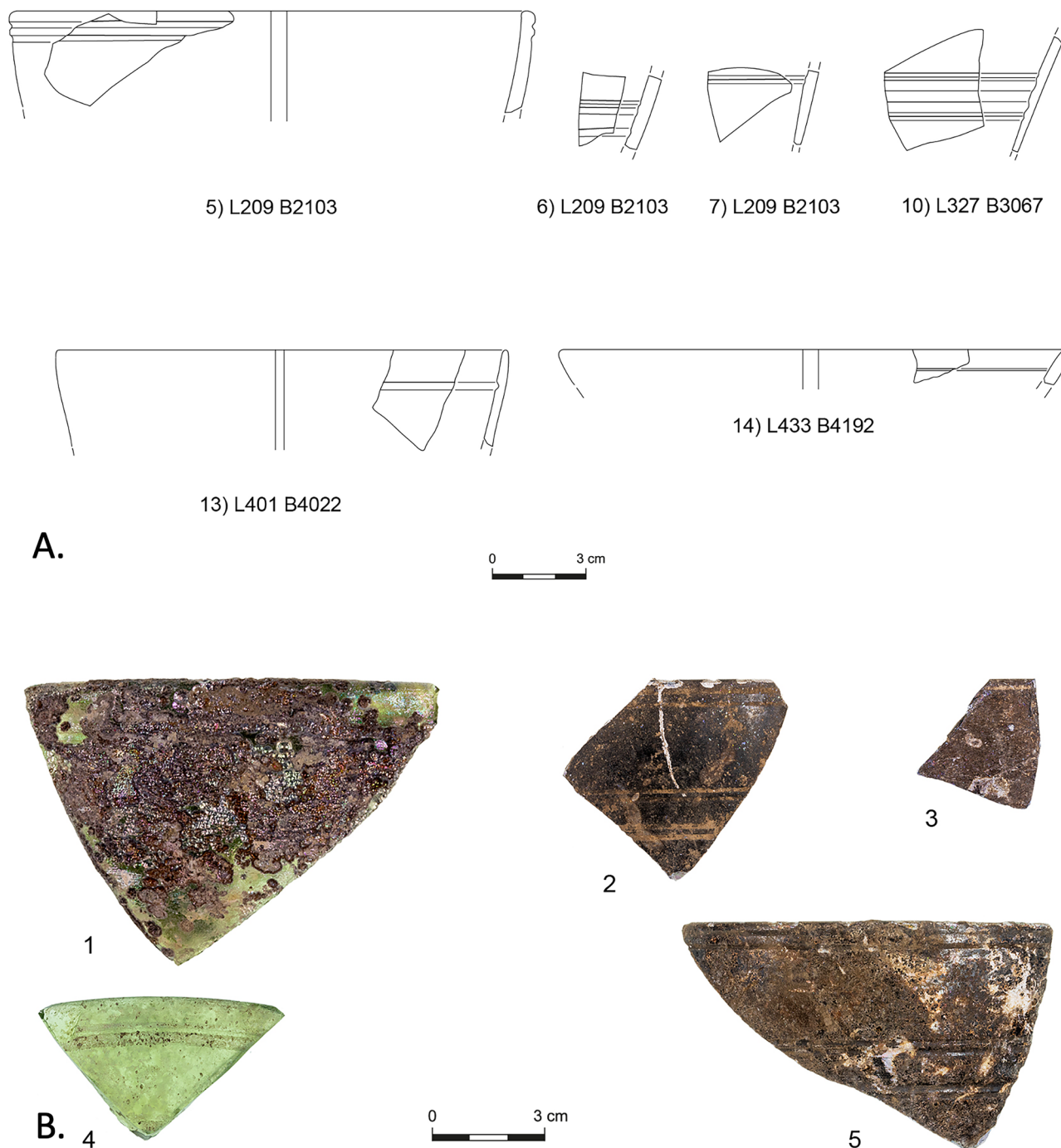


**Fig. 2 | Examples of typology and glass sherds from Tell Izṭabba. A** Drawings of selected shards of glass vessel fragments analysed in this study. **B** Examples of glass vessel fragments similar to the analysed glass shards. Source: German-Israeli Tell Izṭabba Excavation Project (GITIEP).

Georem value =  $0.282865 \pm 0.000013$ ), respectively<sup>21</sup>. Glass standard Corning B ( $n = 13$ ) from Corning Museum yielded  $0.282212 \pm 0.000015$  ( $2 \delta$ ). Monitoring  $^{172}\text{Yb}$ ,  $^{175}\text{Lu}$ ,  $^{181}\text{Ta}$  and  $^{182}\text{W}$  signals throughout the session showed signals were all less than a few mV. Epsilon Hf ( $\epsilon_{\text{Hf}}$ ) was calculated from present-day CHUR values of  $0.28278529$ <sup>22</sup> (Supplementary Data 1).

## Results

### Compositional grouping

The samples in this study classify as soda-lime-silica glass and, more specifically, as natron type glass with  $\text{K}_2\text{O}$  and  $\text{MgO}$  of 0.4 – 1.1 and 0.4 – 0.8 wt%, respectively (Table 2).

Tell Izṭabba base glasses can be divided into two main groups (**IZT-1** and **IZT-2**) based on their  $\text{MgO}$ ,  $\text{Al}_2\text{O}_3$ ,  $\text{FeO}$ ,  $\text{Ti}$  as well as  $\text{Sr}$  and  $\text{Hf}$  isotopic compositions (Fig. 3, Table 2):

**IZT-1** samples ( $n = 26$ ) have homogeneous major element compositions;  $\text{Na}_2\text{O}$   $17 \pm 1$  wt%,  $\text{Al}_2\text{O}_3$   $2.0 \pm 0.1$  wt%,  $\text{CaO}$   $7.8 \pm 0.8$  wt%,  $\text{MgO}$   $0.5 \pm 0.1$ ,  $\text{Ti}$   $306 \pm 31$  ppm and  $\text{FeO}$   $0.27 \pm 0.03$  wt% ( $2 \text{ std dev}$ ; Fig. 3a–c). This group can be further divided into three subgroups based on the use of decolourisers (Table 2 and Supplementary Data 1):

- Subgroup **IZT-1A** includes glasses with no decolourisers ( $n = 4$ ). These glasses have  $\text{Mn}$  and  $\text{Sb}$  concentrations below expected background levels in glassmaking sands ( $< 125$  ppm  $\text{Mn}$  and  $< 5$  ppm  $\text{Sb}$ ).

**Table 2 | Major (wt%) and trace (ppm) compositions for Tell İztabba compositional groups**

	IZT-1						IZT-2	
	IZT-1A		IZT-1B		IZT-1C		m (n = 4)	SD
	m (n = 4)	SD	m (n = 15)	SD	m (n = 7)	SD		
SiO <sub>2</sub>	70.1	0.9	68.6	1.3	67.6	1.3	68.0	1.8
TiO <sub>2</sub>	0.05	0.00	0.05	0.00	0.06	0.01	0.07	0.01
Al <sub>2</sub> O <sub>3</sub>	2.04	0.04	2.07	0.04	2.00	0.07	2.34	0.11
FeO	0.24	0.01	0.27	0.02	0.29	0.03	0.40	0.06
MnO	0.01	0.00	0.45	0.34	0.94	0.25	0.95	0.29
MgO	0.44	0.04	0.53	0.06	0.54	0.03	0.85	0.27
CaO	6.98	0.77	7.87	0.61	8.25	0.59	8.09	0.42
Na <sub>2</sub> O	17.4	0.6	17.3	1.0	17.1	0.4	15.9	1.4
K <sub>2</sub> O	0.63	0.04	0.68	0.07	0.70	0.15	0.82	0.26
Sb	1.89	1.58	8.14	10.90	1443	1299	2536	1976
Cu	5.33	0.35	7.98	2.01	11.0	6.0	16.6	8.9
Pb	14.1	7.5	45.1	44.8	1836	5039	875	1651
Li	2.82	0.06	3.06	0.15	3.24	0.27	3.73	0.37
B	95.6	11.5	107	28	120	41	141	58
Cr	6.97	0.25	7.84	0.53	8.50	0.58	21.4	21.4
Co	0.84	0.03	3.45	2.02	6.75	1.09	10.5	6.8
Ga	2.11	0.06	2.16	0.07	2.10	0.09	2.46	0.12
Rb	9.56	0.88	9.84	1.35	9.65	1.52	9.51	3.17
Sr	390	54	482	37	526	49	509	59
Y	5.87	0.51	6.50	0.41	6.63	0.35	6.30	0.18
Zr	32.3	2.9	32.5	2.4	34.8	2.4	38.8	2.0
Nb	0.96	0.02	1.02	0.06	1.10	0.09	1.40	0.07
Ba	195	6	224	32	232	10	239	24
La	5.06	0.31	5.47	0.25	5.56	0.23	5.71	0.16
Ce	9.25	0.56	9.94	0.50	10.0	0.4	10.4	0.2
Nd	5.21	0.35	5.71	0.27	5.81	0.29	5.83	0.11
Sm	1.03	0.10	1.16	0.07	1.20	0.05	1.20	0.04
Yb	0.49	0.04	0.52	0.03	0.54	0.02	0.54	0.02
Hf	0.78	0.07	0.78	0.06	0.84	0.06	0.93	0.05
Ta	0.06	0.00	0.06	0.00	0.07	0.01	0.09	0.01
Th	0.64	0.02	0.67	0.03	0.71	0.03	0.81	0.11
U	0.67	0.01	0.76	0.24	1.03	0.16	1.17	0.34

SD = one standard deviation.

- Subgroup *IZT-1B* includes glasses with Mn decolouriser only ( $n = 15$ ). These glasses have elevated MnO (0.07–1.2 wt%), while Sb is below or marginally above levels expected in glassmaking sands (up to 42 ppm - in most cases below 10 ppm).
- Subgroup *IZT-1C* includes glasses with both Mn and Sb decolourisers at intentional levels ( $n = 7$ ). These glasses have elevated MnO (0.5–1.3 wt%) as well as Sb (0.06–0.5 wt%) concentrations.

The seven *IZT-1* samples analysed for Hf and Sr isotopic compositions include samples from all three subgroups (two from *IZT-1A*, three from *IZT-1B* and two from *IZT-1C*). The  $\epsilon_{\text{Hf}}$  values range from -8.7 to -12.3 and  $^{87}\text{Sr}/^{86}\text{Sr}$  ratios from 0.708689 to 0.709094, the latter close to the present-day seawater value (Supplementary Data 1). A strong correlation between  $\epsilon_{\text{Hf}}$  and  $^{87}\text{Sr}/^{86}\text{Sr}$  confirms an overall similar origin of the three *IZT-1* subgroups ( $R^2 = 0.76$ ; Fig. 3d).

*IZT-2* ( $n = 4$ ) glasses differ from *IZT-1* glasses by higher MgO (> 0.7 wt%), Al<sub>2</sub>O<sub>3</sub> (> 2.2 wt%), FeO (> 0.4 wt%), Ti (> 400 ppm), Ga (> 2.3 ppm), Ta

(> 0.8 ppm) and Nb (> 1.3 ppm) concentrations (Fig. 3a–c, Table 2, Supplementary Data 1). The two *IZT-2* glasses analysed for Hf and Sr isotopes show these to have relatively lower  $^{87}\text{Sr}/^{86}\text{Sr}$  ratios at a given  $\epsilon_{\text{Hf}}$  value. Thus, the *IZT-2* glasses plot below *IZT-1* glasses in  $\epsilon_{\text{Hf}}$  -  $^{87}\text{Sr}/^{86}\text{Sr}$  space (Fig. 3d).

### Sample pairs

A number of samples have compositions that are more-or-less within experimental error for all elements. These could potentially represent fragments from the same vessel or vessels from the same production event (batch)<sup>23–25</sup>. The identified samples are: colourless glasses Tell İz-7, Tell İz-13 and Tell İz-14; amber tinted glasses Tell İz-5 and Tell İz-6; yellowish glasses Tell İz-20 and Tell İz-29 as well as amber tinted glasses Tell İz-22, Tell İz-23 and Tell İz-26 (Supplementary Data 1). Where they are from different loci in the excavation, they likely represent different vessels from the same batch, but two pairs of samples (Tell İz-5 and Tell İz-6; Tell İz-22 and Tell İz-23) comprise samples from the same locus, which may represent fragments of a single vessel. The sample pairs are shaded blue in Supplementary Data 1. If it

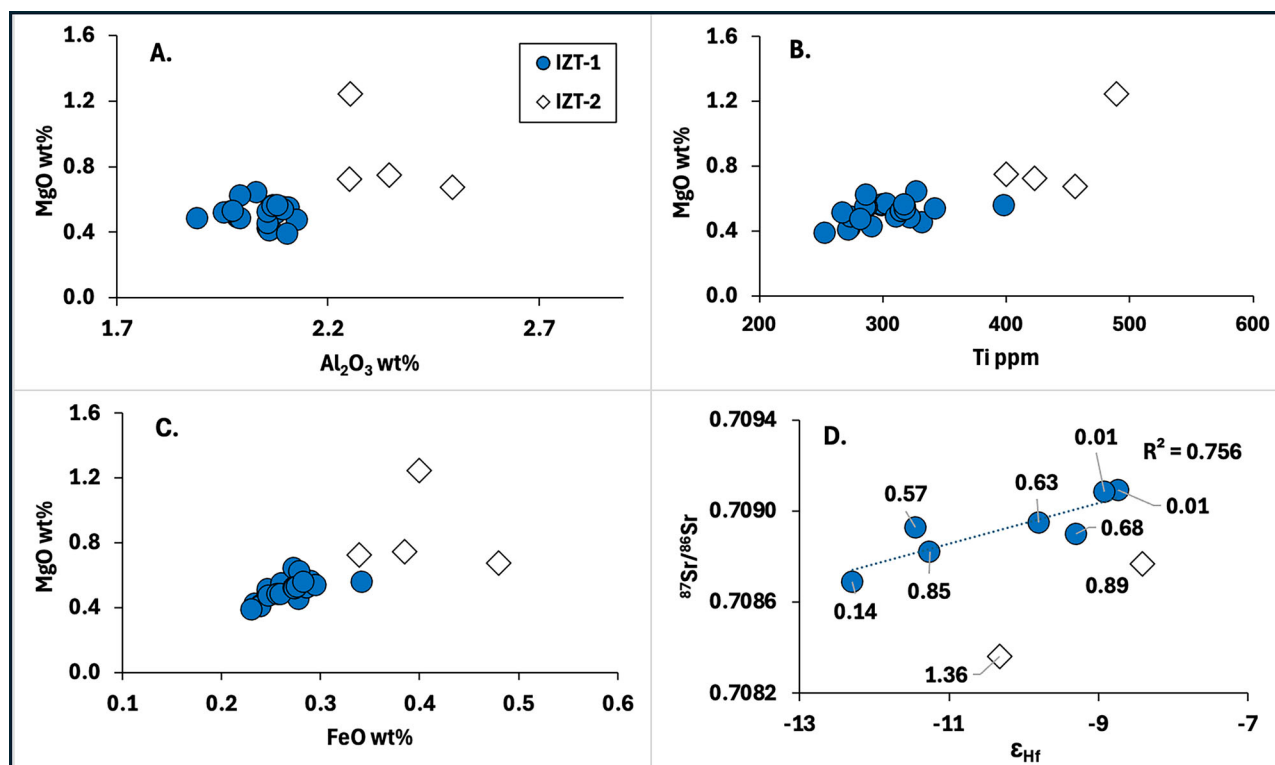


**Fig. 3 | Examples of typology and glass sherds from Tell Iztabba.** MgO versus A.  $\text{Al}_2\text{O}_3$  (wt%) B. Ti (ppm) and C. FeO (wt%) showing the differences between the two glass types at Tell Iztabba illustrated by relatively elevated concentrations of MgO,  $\text{Al}_2\text{O}_3$ , FeO and Ti observed for IZT-2 relative to IZT-1 samples. D.  $^{87}\text{Sr}/^{86}\text{Sr}$  versus

$\epsilon_{\text{Hf}}$  showing the lower  $^{87}\text{Sr}/^{86}\text{Sr}$  ratios at a given  $\epsilon_{\text{Hf}}$  value for IZT-2 glasses. For  $^{87}\text{Sr}/^{86}\text{Sr} - \epsilon_{\text{Hf}}$  plot, data points are labelled with MnO concentrations showing that the different isotopic values observed for IZT-1 relative to IZT-2 samples are independent of added Mn decolouriser.

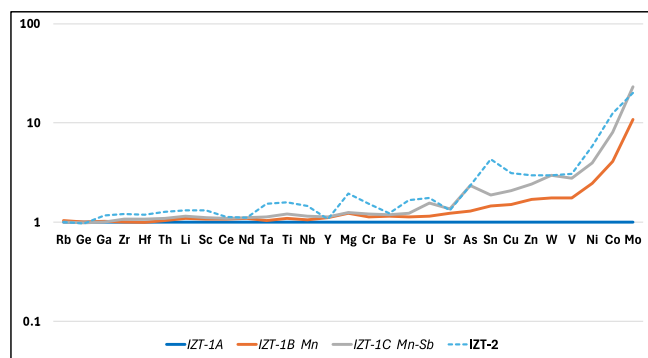


**Fig. 4 | Trace element characteristics for Tell Iztabba glass groups.** Mean concentrations of trace elements within the Tell Iztabba subgroups IZT-1B and IZT-1C and main group IZT-2 normalised to mean concentrations for subgroup IZT-1A. Note that high Cr concentration (53 ppm) for sample Tell Iz-1 was excluded from the average of IZT-2 glasses. Data from Supplementary Data 1.

is assumed that all sample pairs represent the same vessels, then the ‘true’ number of samples in each subgroup/group would be IZT-1A (3), IZT-1B (12), IZT-1C (5) and IZT-2 (4).

**Compositional effects from decolourisers**

Figure 4 compares the mean concentrations of trace elements observed for IZT-1 subgroups IZT-1A (no decolourisers), IZT-1B (Mn decolouriser) and IZT-1C (Mn and Sb decolourisers), as well as for main group IZT-2 glasses (Mn and Sb decolourisers). By normalising to the mean values for IZT-1A glasses which are devoid of decolourisers, it appears that IZT-1 subgroups share the same sand source given the similar concentrations and proportions of rare earth elements (REE), Rb, Ge, Ga, Zr, Hf, Th, Li, Sc, Ta, Ti, Nb,

Y, Mg and Cr, as these are expected to have been derived primarily from glass-making sands. For these trace elements in IZT-1 glasses, coefficients of variation (= relative standard deviation, RSD) are typically around 8% or lower (except for Rb and Ge with RSDs of 13 and 15%, respectively), as are RSDs for base glass major oxides, which are below 5% for  $\text{SiO}_2$ ,  $\text{Al}_2\text{O}_3$  and  $\text{Na}_2\text{O}$  (Supplementary Data 1).

In contrast, V, Co, Ni, Cu, Zn, As, Mo, and Ba vary significantly between the IZT-1 subgroups (Fig. 4) and have elevated RSDs of 35-78%. Positive correlations with manganese or antimony show that these were likely impurities in the ores<sup>26,27</sup> (Fig. 5). This accounts for their significantly elevated concentrations in the subgroups IZT-1B and IZT-1C where antimony and/or manganese have been added as decolourants (Fig. 4, left). Strong linear correlations of MnO with elements, such as V, Ni, Co, Mo and Ba ( $R^2 > 0.8$ ; Fig. 5a, b) suggest a single source of manganese ore was used for the IZT-1 glasses. Furthermore, the use of the same manganese ore is suggested for IZT-2 glasses given that they fall on the same trends (Fig. 5a, b).

Antimony oxide,  $\text{Sb}_2\text{O}_5$ , is present at technologically significant levels only in samples belonging to subgroup IZT-1C as well as in IZT-2 glasses, ranging from c. 400 ppm to 0.62%. Within these groups, Sb correlate with As, as might be expected (Fig. 5c). Weaker correlations occur between Sb and a number of other elements, including Sn, Cu and In (Fig. 5d). Lead oxide is typically below 60 ppm, but on occasion clearly represents deliberate addition, ranging up to 1.34% PbO in one vessel. The three samples with lead above 200 ppm exhibit elevated antimony, an association noted elsewhere<sup>28</sup>. Bismuth is strongly correlated while tin and indium tend to correlate with lead, perhaps suggesting the use of scrap lead metal including small amounts of the lead-tin alloy, pewter.

**The effects on Sr concentration and isotopic composition from decolourisers**

Compared to the strong correlations of Ni, Mo and Ba discussed above, manganese shows only a modest correlation with strontium (Fig. 6a).

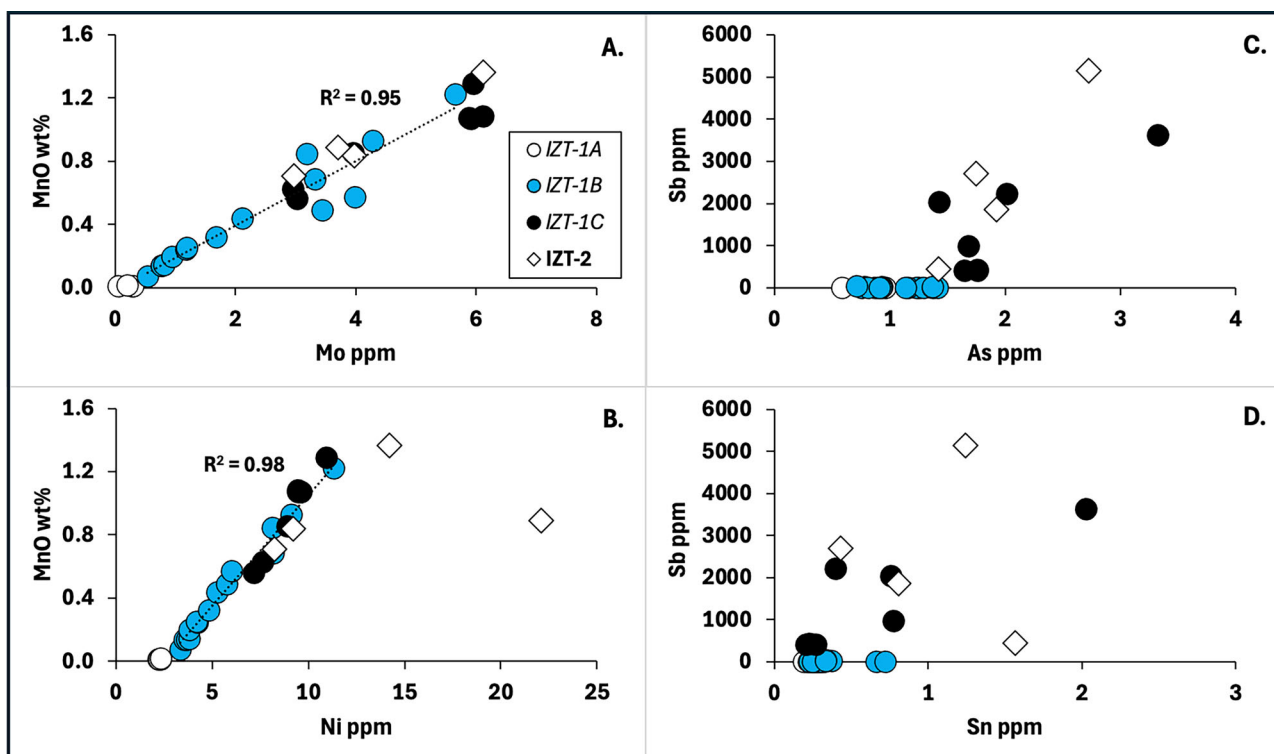


**Fig. 5 | Composition influence from Mn and Sb decolourisers.** Correlations of (A). Mo versus MnO, (B). Ni versus MnO, (C). As versus Sb and (D). Sn versus Sb for the glass subgroups IZT-1A, IZT-1B and IZT-1C and group IZT-2.

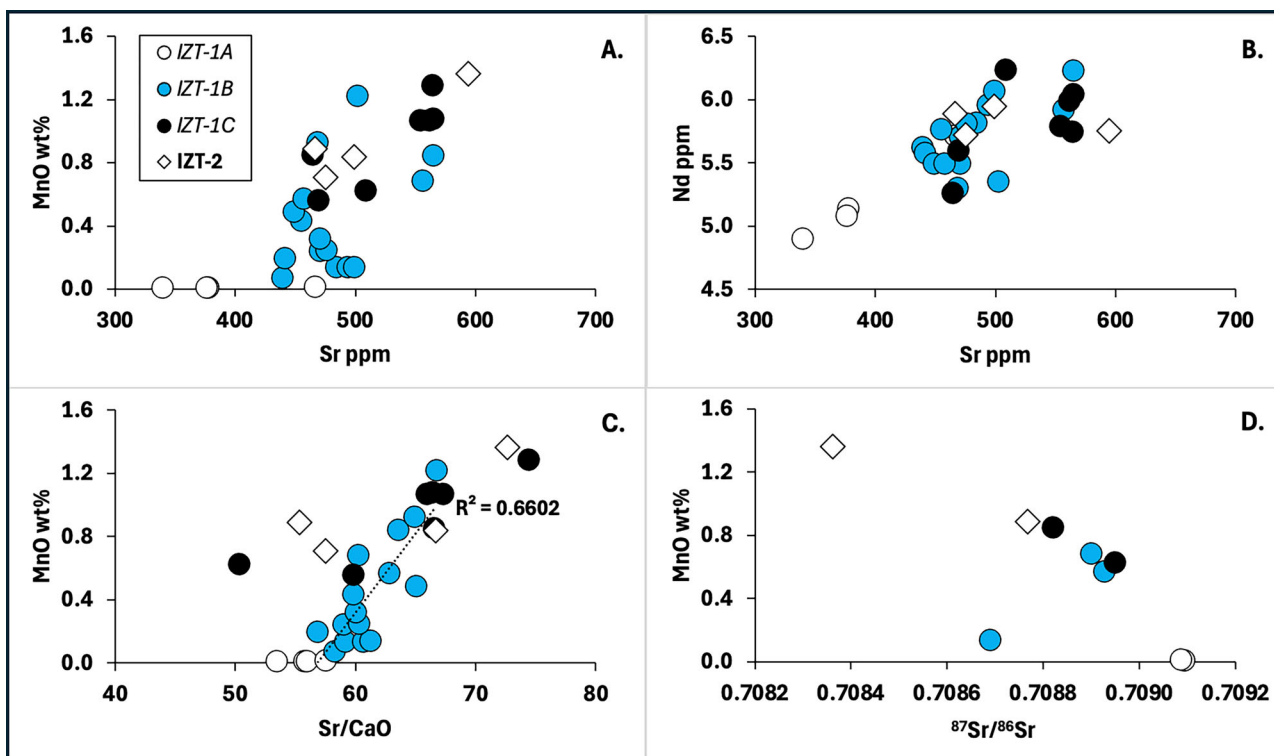


**Fig. 6 | Controls on Sr concentration and  $^{87}\text{Sr}/^{86}\text{Sr}$  ratio.** The control from addition of decolourant (pyrolusite  $\text{MnO}_2$ ) on A. Sr concentrations and B. Sr/Ca ratios for the Iztabba glasses. C. Nd versus Sr showing a competing control on Sr concentrations and D. MnO versus  $^{87}\text{Sr}/^{86}\text{Sr}$  ratio.

Although strontium thus is implied to have been somewhat affected by the addition of manganese ore, as discussed in previous studies<sup>29,30</sup>, it is also controlled by other primary processes relating back to the raw materials. For instance, strontium concentrations show a strong dependence on neodymium concentrations—particularly for glasses with low manganese—as also shown for 4th century natron glass from Jalame<sup>27,31</sup> (Fig. 6b).

<sup>87</sup>Sr/<sup>86</sup>Sr isotope ratios were determined for nine glasses and range between 0.7084 and 0.7091, which is within the range generally found for eastern Mediterranean natron glass made using coastal sands<sup>30,32,33</sup>. Within this range they are dependent upon the Sr/Ca ratio which itself is dependent upon the addition of manganese (Fig. 6c). Samples with low Mn and low Sr approach most closely the isotopic ratio of Holocene sea water (aragonitic shell; <sup>87</sup>Sr/<sup>86</sup>Sr = 0.7092<sup>34</sup>). However, we also observe ‘competing’ controls on the strontium isotopic concentration of the Tell Izṭabba glasses. Firstly, glass sample Tell Iz-22 from the *IZT-1B* subgroup has a low <sup>87</sup>Sr/<sup>86</sup>Sr ratio of 0.7087, but also a low MnO content (0.14 wt%; outlier in Fig. 6d). This therefore represents a natural, ‘low’ strontium isotopic composition originating from primary glassmaking materials. Secondly, Sr and Hf isotopic compositions correlate independently of manganese (and to a higher degree;  $R^2 = 0.76$ ; Fig. 3d).

## Discussion

The virtually identical sand-related elements in Fig. 4 (to the left of Mg) for the *IZT-1* subgroups confirm that these were made from raw glass from the same primary production, irrespective of differences in manganese and antimony contents (section 3.3). *IZT-2* glasses have elevated sand-related elements, in particular, higher Ta, Nb and Cr in addition to the already noted higher Al<sub>2</sub>O<sub>3</sub>, TiO<sub>2</sub>, FeO and MgO concentrations. It seems likely therefore that *IZT-2* glass was made from different sands and thus produced in a different location.

The  $\epsilon_{Nd}$  values for two samples from each of the groups (*IZT-1* and *IZT-2*) from Tell Izṭabba range from -4.3 to -4.8, while the Sr isotopes are typically close to seawater values (0.7092<sup>34</sup>; Fig. 7a, b). The strontium and neodymium isotope measurements thus are fully consistent with an origin for the Tell Izṭabba glass on the Eastern Mediterranean coast, either in the Levant or in Egypt<sup>29,33,35</sup>. In terms of TiO<sub>2</sub>/Al<sub>2</sub>O<sub>3</sub> and Al<sub>2</sub>O<sub>3</sub>/SiO<sub>2</sub> ratios, *IZT-1* glasses overlap with Roman-Sb glass, considered to have been made in Egypt<sup>21</sup> and *IZT-2* glasses with manganese-decoloured Roman-Mn glass from the Levant (Fig. 8). The overlap of *IZT-1* with the field of Egyptian Roman-Sb glass is unexpected, given the strong Levantine association of monochrome cast bowls.

There is no observable change in Hf isotopic compositions with MnO (Fig. 3d) showing that the addition of decolourisers did not significantly affect  $\epsilon_{Hf}$  values. Hafnium isotope compositions for seven *IZT-1* and two *IZT-2* glasses have  $\epsilon_{Hf}$  values that range between -8.4 and -12.3. This spread for the Hellenistic bowls is wider than any other coherent group analysed for hafnium isotopes and includes the most depleted (least negative)  $\epsilon_{Hf}$  values so far observed for historical glass (Fig. 7c).

Previous work on hafnium isotopic of ancient glass<sup>21,27</sup> has shown that glass made from Egyptian sands has  $\epsilon_{Hf}$  values that are lower (more negative) than glass made from Levantine coastal sands. The division between the two regions was shown to be at around  $\epsilon_{Hf}$  of -12.5, with more negative values comprising the Egyptian glass types Rom-Sb, Foy 2.1 and Egypt 1<sup>21</sup>. On this basis, both groups of Tell Izṭabba Syro-Palestinian bowls, which have  $\epsilon_{Hf}$  values consistently greater than -12.5, and typically lie well into the Levantine range, are considered to have been made from sands on the Syro-Palestinian coast, rather than Egyptian sands (Fig. 7c). This resolves the apparent discrepancy between the Egyptian affiliation of *IZT-1* suggested by its low Al<sub>2</sub>O<sub>3</sub>/SiO<sub>2</sub> ratio and the Levantine character of the glass forms; the glass is indeed of Levantine origin and the fields shown in the discrimination diagram (Fig. 8), based upon Roman and later glass, are not appropriate for glass from earlier periods.

Even so, the wide range of  $\epsilon_{Hf}$  values requires further discussion. The regional differences imply that the sands from Egypt contain a heavy mineral assemblage in which the zircons have mean geological ages that are

older (= more negative  $\epsilon_{Hf}$  values) than the zircons in Levantine sands<sup>36</sup>. We have previously noted that an explanation for the less radiogenic  $\epsilon_{Hf}$  composition of glass (< -12.5) from the Levantine coast is that zircons of different size are sorted by hydraulic processes as the sand is moved round the Mediterranean coast from the Nile<sup>21</sup>. This process is evident in that the zirconium levels in Egyptian glass are in general significantly higher than in Levantine glass<sup>37</sup>. Thus, the hafnium isotope values are considered a robust indicator of Levant versus Egyptian source as they reflect differences in the regional geochemistry. The wider range of  $\epsilon_{Hf}$  (-8.4 to -12.3) observed in Tell Izṭabba may reflect the production of glass in smaller batch sizes in the Hellenistic period, and possibly more dispersed primary production, leading to an apparently higher heterogeneity.

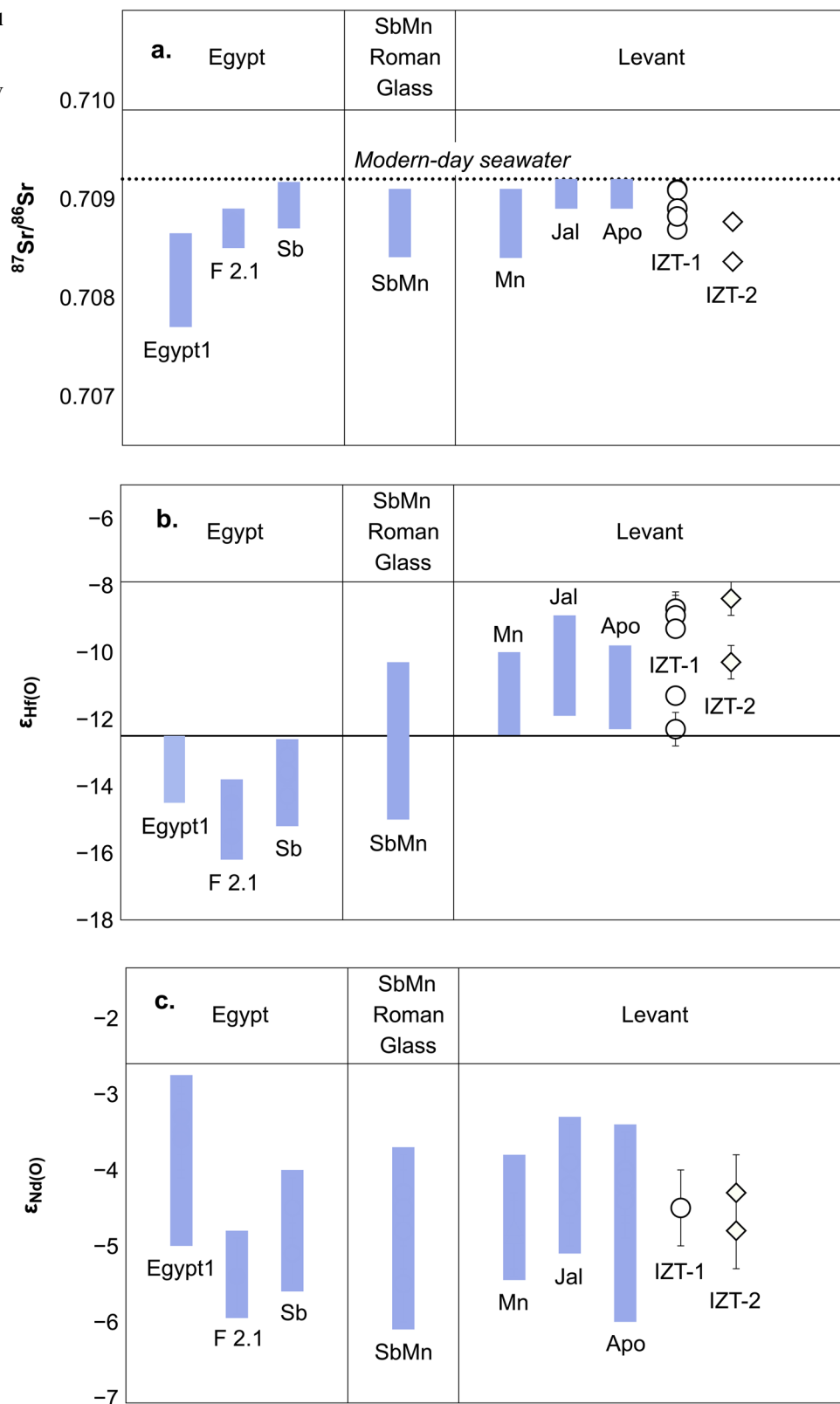
Alumina contents for Tel Izṭabba glass are compared with various other glass groups in Fig. 9. It is noteworthy that the *IZT-1* glass group has mean Al<sub>2</sub>O<sub>3</sub> values (2.05 ± 0.06 wt%) that are lower, while *IZT-2* glass have Al<sub>2</sub>O<sub>3</sub> values (2.34 ± 0.11 wt%) that are similar to Roman Levantine glasses as represented by late Hellenistic (first century BCE) and early Roman hemispherical bowls from Beirut<sup>38</sup>, Roman-Mn type glass from Carthage<sup>39</sup>, London<sup>27</sup> and Jerash<sup>26</sup> as well as Roman-Mn colourless glass from the shipwreck *Iulia Felix*<sup>40</sup>. The *IZT-2* type glasses furthermore group with Roman-Mn glasses in Fig. 8, so we can be reasonably confident that the difference between *IZT-1* (Hellenistic) glass and Roman-like glass is real. This observation serves to emphasise the division between *IZT-1* and *IZT-2*.

Data sets exist for Jalame type glass from Carthage<sup>39</sup>, Jerash<sup>26</sup> and from the production site at Jalame<sup>27</sup>, for Apollonia type glass from production at Apollonia<sup>41,42</sup>, Jerash<sup>26</sup> and various sites in Israel<sup>43</sup> and, finally, for Beth Eli'ezer type glass<sup>41,43</sup>. These three types are all characterised by relatively elevated Al<sub>2</sub>O<sub>3</sub> values (Al<sub>2</sub>O<sub>3</sub> > 2.8 wt%) and are known to have been produced to the south of Haifa on the Levantine coast.

It has previously been observed that Levantine Roman glass found in Europe (i.e. Roman-Mn) has lower Al<sub>2</sub>O<sub>3</sub>/SiO<sub>2</sub> than glass made in known primary furnaces from Israel, i.e., Apollonia, Beth Eli'ezer, Beth She'arim and Jalame<sup>27</sup>. On this basis it was suggested that the source of the glass-making sand was around or North of Carmel, perhaps Akko-Ptolemais, Sidon or Beirut, where literary reference<sup>44</sup> and archaeological evidence<sup>45</sup> suggest glass manufacture in the early Roman period. A single analysis from the furnaces in Beirut<sup>14</sup> supports this model, while data on sediments off the coast of Israel also show a clear decrease in Al<sub>2</sub>O<sub>3</sub> from south to north, although there are no data for the sands of the coast north of the Bay of Haifa<sup>46</sup>. The present evidence therefore suggests that the low-alumina glass of the *IZT-1* Tel Izṭabba bowls originated to the North, on the coast of modern Lebanon. If the general decrease in the alumina content of sand (and hence primary glass) continues up the Lebanese coast, then it might be predicted that the manufacturing centre for Hellenistic glass of the *IZT-1* type was north of Beirut, perhaps centred on a Phoenician city, such as Byblos. The higher alumina of *IZT-2* glasses, however, is similar to early Roman glass, suggesting that it was made in Beirut. Thus, the Tell Izṭabba assemblage appears to span the period of transition between typical late Hellenistic and early Roman primary productions, rather than two fully contemporaneous Hellenistic glass productions.

Oikonomou et al.<sup>47</sup>, although dealing with earlier, core-formed material, suggest multiple sources for Hellenistic glass, and the differences observed here could be considered consistent with this view. Hellenistic monochrome glass from Jebel Khaled, Syria, dated late 2nd–early 1st centuries BCE, has a much larger range of Al<sub>2</sub>O<sub>3</sub> concentrations (1.04 to 2.58 wt %; 2.19 ± 0.26) that range to a much higher degree than for the Tell Izṭabba glass<sup>48</sup>. Thus, the Jebel Khaled assemblage is likely to include several glass groups. Given our classification using relatively low levels of MgO, FeO and Ti (Fig. 3) and the fact that comparisons of Al<sub>2</sub>O<sub>3</sub> values at the 0.1% level can be misleading due to the use of different analytical techniques (SEM-WDS versus LA-ICPMS) along with potential systematic errors, we have not attempted to subdivide the Jebel Khaled glasses into subgroups and thus have not included these in Fig. 9. Even so, it appears that glass of the *IZT-1* type is present at Jebel Khaled.

**Fig. 7 | Hf, Sr and Nd isotopic compositions of Tell Izṭabba glass. A. Sr, B. Hf and C. Nd isotopic compositions for IZT-1 and IZT-2. Comparative groups are, from left to right: Egypt 1 (Egypt1), Foy 2.1 (F 2.1), Roman-Sb (Sb), Recycled Roman (SbMn), Roman-Mn (Mn), Jalame (Jal), Apollonia (Apo)<sup>20,26</sup>.**



The Tell Izṭabba samples are ranked by manganese content in Fig. 10a, which shows the relationship of MnO content to colour. Colourless glass is high in MnO, while yellowish/amber and bluish glasses have low and greenish glasses have intermediate MnO concentrations. This is consistent with the addition of manganese oxide as a decolouriser<sup>11,49</sup>, probably as pyrolusite, MnO<sub>2</sub>. The decolouriser acted as an oxidising agent which

converted Fe<sup>2+</sup>, which imparted a strong blue, into pale yellow Fe<sup>3+</sup> which, in thin-walled glass vessels appeared colourless. Amber glass, with a low oxidation state, typically has low manganese, while colourless glass, which requires the iron to be oxidised, has high manganese, demonstrating very clearly the principle. Bluish glass, where most of the iron is anticipated to be in the reduced Fe<sup>2+</sup> state, has a lower manganese content than greenish glass,

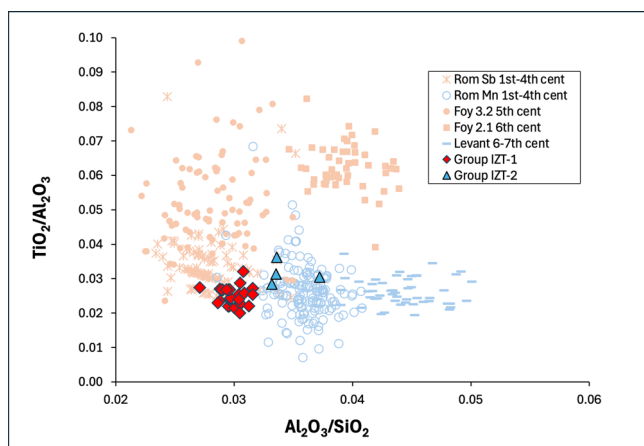


**Fig. 8 | Natron glass types in the first millennium CE.** Division of IZT-1 and IZT-2 samples and comparison with key primary glass reference groups of the first millennium CE. Egyptian reference groups shown in orange and Levantine in blue. Note that even though IZT-1 samples plot in Roman-Sb, their Hf isotopic values exclude an Egyptian origin. Reference data sources include <sup>37-40,43,51,58</sup>.

where more iron is present as the Fe<sup>3+</sup> yellowish cation. These observations generally fall into previously observed patterns from late Roman Levantine glass (4th cent CE) at Jalame<sup>27</sup> and early Roman glass (1st cent BCE-1st cent CE) from Beirut<sup>38</sup>.

Of particular interest is that the Tell Iẓṭabba samples tend to be more consistently oxidised than the later Beirut glasses, so that at Iẓṭabba few glasses with more than 0.6% MnO are coloured and all glasses above 1% MnO are colourless. At Beirut, on the other hand, glass with over 1% MnO is frequently tinted<sup>38</sup>. While the determination of weak tints in glass is a relatively subjective procedure, depending on the perception of the viewer and the thickness of the piece being examined, in the present case the differences are quite pronounced and we believe are likely to be significant, as discussed below.

A particular characteristic of the Iẓṭabba glasses is that many of them contain antimony, the other decolouriser of antiquity, in addition to manganese. Figure 10b compares antimony and manganese contents in the bi-plot used by other authors when considering Roman glass<sup>50</sup>. It is observed that all colourless glasses contain both manganese and antimony, with one exception (Tell Iz-25) which has a very high MnO content of 1.2 wt%. Weak colours contain only manganese, or insignificant concentrations of both decolourisers. This probably explains the very consistent occurrence of colourless glass observed in the Iẓṭabba assemblage (Fig. 10b), as the presence of antimony will have supplemented the decolourisation effect of the manganese.

The occurrence of manganese and antimony together in Roman glass of the first century CE onwards is generally considered to be the result of the mixing of two glasses during recycling: an Mn-decolourised endmember (Rom-Mn) made in the Levant and an Sb-decolourised endmember (Rom-Sb) made in Egypt<sup>26,51-54</sup>. In a Sb-Mn bi-plot for Roman glass, of the type shown in Fig. 10b, the Sb-decolourised Egyptian glasses are typically spread on the vertical axis, the Levantine Mn-decolourised glasses along the horizontal axis and the recycled glasses lie in a broad mixing zone between them. However, the Iẓṭabba glass shows a very different pattern. All glass appears to be of Levantine origin and there is no evidence of an Sb-rich endmember glass in the assemblage – there are no glasses containing intentionally-added Sb without intentionally-added Mn. Furthermore, all glasses in which Sb is significantly above background (> 10 ppm Sb) contain at least 0.5 wt% MnO. The base compositions of the two Iẓṭabba compositional groups are distinct and both groups conform to the pattern of Sb and Mn occurrence observed. We therefore conclude that the occurrence of antimony and manganese in the same samples in the Iẓṭabba glass is not the result of glass mixing or recycling but of the deliberate decolourisation of individual glass batches with both antimony and manganese.

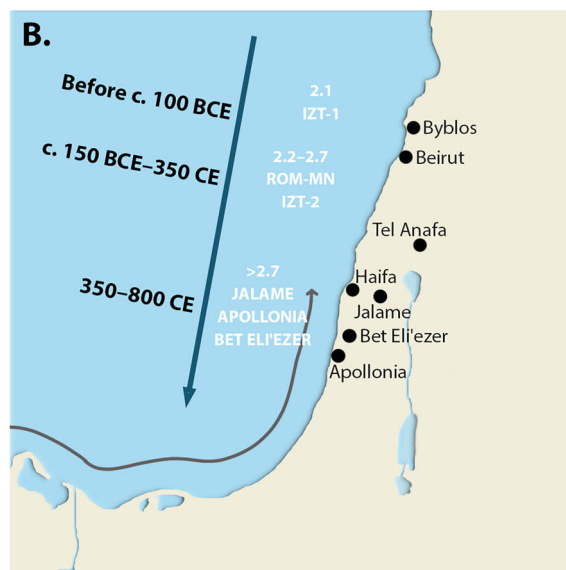
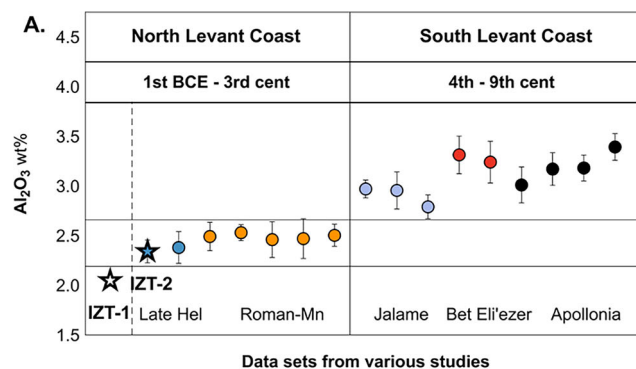


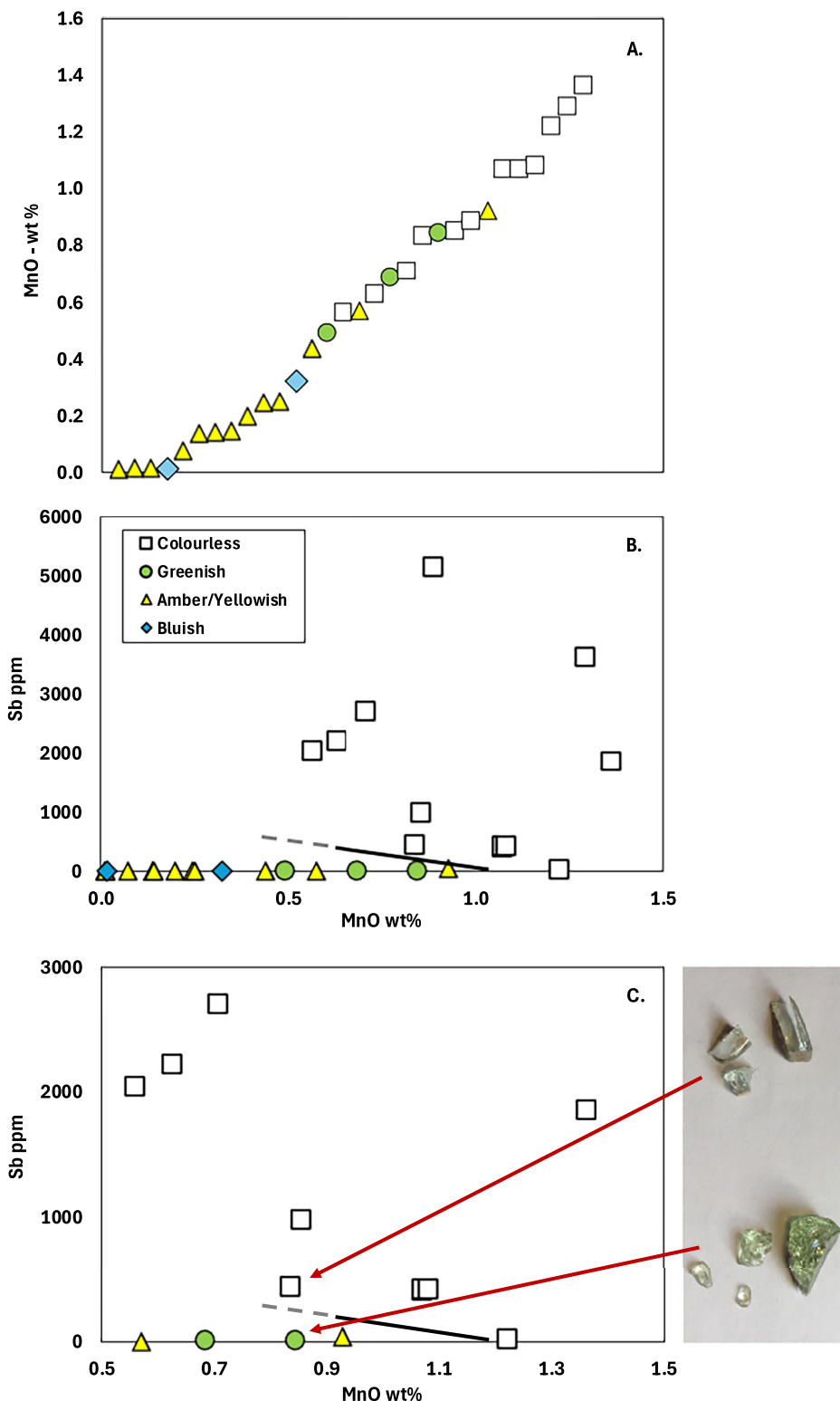
**Fig. 9 | Chronological shift in Al<sub>2</sub>O<sub>3</sub> from north to south on the Levantine coast.**

Our proposed model for a chronological shift from North to South in glass production sites along the Levantine coast based on a systematic decrease in Al<sub>2</sub>O<sub>3</sub> contents. **A.** From left - Mean Al<sub>2</sub>O<sub>3</sub> values for IZT-1 glass from Tell Iẓṭabba (> 1st cent BCE; star), compared to data sets for late Hellenistic (IZT-2 from Tell Iẓṭabba; blue star, and late Hellenistic glass from Beirut<sup>38</sup>; blue circle) and 1st BCE - 3rd centuries Roman-Mn glass from Beirut<sup>38</sup>, Carthage<sup>39</sup>, London<sup>27</sup>, Jerash<sup>26</sup> and Iulia Felix<sup>40</sup> (orange circles). Data sets for 4<sup>th</sup> century CE Jalame type glass recovered from Carthage<sup>39</sup>, Jerash<sup>26</sup> and Jalame<sup>27</sup> (purple circles), from 8<sup>th</sup> century CE Bet Eli'ezer glass<sup>41,43</sup> (red circles) as well as for 6-7th century CE Apollonia type glass recovered from glass production at Apollonia<sup>41,42</sup>, Jerash<sup>26</sup> and various sites in Israel<sup>43</sup> (black circles). Error bars represent ± 1 std dev. Note that symbol for the IZT-1 data set is larger than error bars. **B.** Map showing the geographical and proposed chronological increase in Al<sub>2</sub>O<sub>3</sub> content observed for glass types produced from north to south along the Levantine coast. Known glass production sites on the South Levantine coast have Al<sub>2</sub>O<sub>3</sub> > 2.8 wt% while lower Al<sub>2</sub>O<sub>3</sub> in late Hellenistic and Roman-Mn type glasses with Al<sub>2</sub>O<sub>3</sub> = 2.2-2.7 wt% imply production near Beirut. Based on lower Al<sub>2</sub>O<sub>3</sub> (Al<sub>2</sub>O<sub>3</sub> = 2.05 wt%) observed for IZT-1 type glasses, the implication is that these would have been produced further to the north of Beirut.

Given that the manganese contents of the Iẓṭabba glasses are essentially a continuous range from background sand levels of 1-200 ppm through to over 1 wt % (Fig. 10a, b), it seems likely that the manganese additions were made at the primary glassmaking stage, as has been argued for later glass at Jalame, for example<sup>27</sup>. However, if Sb and Mn were added together in a single decolourisation event, it is difficult to understand why significant antimony concentrations appear confined to glass with more than 0.5% MnO (Fig. 10b). Instead, it seems likely that antimony was added to modify the colour of glass which already contained manganese, and to make a less tinted ("more colourless") glass. Figure 10a shows that above 0.5% MnO,

**Fig. 10 | Decolourisation process at Tell Iztabba.**

A. Tell Iztabba samples are ranked by manganese oxide content and labelled according to colour. B. Manganese oxide versus antimony showing that how manganese has led to amber-yellowish, bluish and greenish colours for the Tell Iztabba glasses, while it is only the combination of antimony and manganese that led to colourless appearances. Only exception is colourless sample Tell Iz-25 with highly elevated MnO = 1.22 wt% and no Sb. White squares = colourless, blue circles = bluish, green circles = greenish and yellow triangles = yellowish/amber samples. C. A closer look at Sb versus MnO shows the dramatic difference in ‘colour’ for samples Tell Iz-18 (greenish) and Tell Iz-17 (colourless) with near-identical MnO and FeO concentrations of 0.85 wt% and ~ 0.3 wt%, but different Sb concentrations of 7 ppm and 436 ppm, respectively.



green-tinted colours begin to occur. It therefore seems likely that the artisans added antimony to green tinted glass to make it appear colourless, or to reduce the tint of near-colourless glass. It seems that amber glasses were so reduced that no attempt was made to decolourise them, as it would have required too much antimony, which is likely to have been expensive, and because amber was itself a desired colour, used frequently in Hellenistic glass bowls. Instead the antimony additions were a product improvement technique, to decolourise weakly tinted glass. It is unclear precisely at which stage

in the chaîne opératoire the antimony additions were made. It could have been at a second stage in the primary glassmaking workshop, or immediately prior to glass working in the secondary workshop. In any event, the craftspeople were clearly skilled at adding appropriate amounts of antimony to decolourise the glass, presumably via a trial-and-error titration-like process.

A final observation is that, based on the present small sample, the Iztabba Group IZT-2 colourless glasses tend to have more antimony than

those of **IZT-1**. This may be because the iron contents of **IZT-2** glasses (0.34–0.48% Fe<sub>2</sub>O<sub>3</sub>) are higher than those of Group 1 (0.24–0.34% Fe<sub>2</sub>O<sub>3</sub>) and a higher level of decolouriser was therefore required. We cannot, however, rule out the possibility that antimony was more accessible to the makers of **IZT-2** glass.

In summary, the analysis of the late second century BCE glass assemblage of monochrome glass bowls from Tell Izṭabba, dated no later than 107 BCE, has provided insights into two major changes which underpin the massive expansion in glass production of the imperial Roman period.

Two compositional groups are present in the assemblage. Group **IZT-1** is distinct from Roman glass made in the Levant, by low contents of Al<sub>2</sub>O<sub>3</sub>, TiO<sub>2</sub>, FeO and MgO. Group **IZT-2**, represented by four samples, closely resembles the well-known Roman-Mn glass, which in turn is similar to primary glass produced in Beirut<sup>38</sup>. Comparison with literature has confirmed this general difference between Hellenistic (**IZT-1**) type and early Roman (**IZT-2**) glass. The present data suggest that the change in glass composition occurred at the end of 2nd century BCE. In view of the apparent general decline of alumina in sands going north along the eastern Mediterranean coast (Fig. 9), we suggest that the manufacture of raw **IZT-1** glass took place in or close to one of the Phoenician cities to the North of Beirut. It is unclear whether the manufacture of both glass groups overlapped but given the low numbers of the later “Roman-like” **IZT-2** group, we suspect that the move in production location occurred towards the end of the 2nd century BCE as represented by the Tell Izṭabba assemblage.

The second change which appears to be represented in the assemblage by a decolourisation technique from the use of antimony to the use of manganese oxide. At Tell Izṭabba antimony is significantly above background levels in colourless glasses only. This appears to reflect a second stage of decolourisation where antimony was added to glass which already contained manganese. Manganese was probably added at the primary production stage, as in later glasses at Jalame. However, this produced batches of glass with variable Mn contents and a wide range of colours. Antimony was added to transform the imperfectly decolourised Mn-containing glass into the desirable colourless material. This approach appears to be characteristic of both compositional groups, **IZT-1** and **IZT-2**. Furthermore, trace elements indicate that both productions used similar sources of manganese and antimony.

By the late 1st century BCE, the practice of adding antimony to decolourise glass seems to have ceased in the Levant and primary Levantine glass contains only manganese, a situation which appears to be maintained through to the 4th century CE. However, the more expensive Egyptian glass decolourised with antimony appears in the second half of the 1st century CE<sup>38,54,55</sup>. The result was that the two regions specialised, with the Levant producing a cheaper product typically tinted blue-green and less commonly colourless while Egypt produced more expensive colourless glass containing antimony (Alexandrian glass), as is attested in the Diocletian Edict<sup>56,57</sup>. Tell Izṭabba records an earlier intermediate practice, whereby antimony was used to modify the colour of glass already decolourised to a greater or lesser extent by manganese.

Overall, we have identified a previously unrecognised shift in production location, distinguishing the majority of Hellenistic from Roman glass, as well as a previously unrecognised decolourisation technology, involving the addition of antimony to manganese-decolourised glass. This study illustrates the power of comprehensive geochemical analysis, including hafnium isotopes, to produce new insights into ancient glass production when applied to a contextually secured and chronologically constrained assemblage.

## Data Availability

All data are contained within the figures of the manuscript and can be downloaded from Supplementary Data 1–3.

Received: 29 August 2025; Accepted: 28 October 2025;

Published online: 24 November 2025

## References

- Jackson-Tal, R. E. The late Hellenistic glass industry in Syro-Palestine: a reappraisal. *J. Glass Stu.* **46**, 11–32 (2004). <https://www.jstor.org/stable/24190927>.
- Grose, D. F. The Pre-Hellenistic, Hellenistic, Roman and Islamic glass vessels in Tel Anafa, Volume II, ii: Glass Vessels, Lamps, Objects of Metal, and Groundstone and Other Stone Tools and Vessels (eds. Berlin, A. M. & Herbert, S. C.) 1–98 (Ann Arbor, 2012).
- Foy, D. Une production de bols moulés à Beyrouth à la fin de l'époque hellénistique et le commerce de ces verres en Méditerranée occidentale. *J. Glass Stud.* **47**, 11–35 (2005).
- Jennings, S. Vessel Glass from Beirut, BEY006, 007, and 045 (Berytus Archaeological Studies 48–49, 2004–2005) (Beirut, 2006).
- Jackson-Tal, R. E., Lichtenberger, A. & Tal, O. Hellenistic vitreous finds from Seleucid Tell Izṭabba. *Levant* **52**, 382–392 (2020).
- Barag, D. P. Catalogue of Western Asiatic Glass in the British Museum, I (London, 1985).
- Grose, D. F. The Syro-Palestinian glass industry in the later Hellenistic period. *Muse* **13**, 54–65 (1979).
- Bettineschi, C. & Angelini, I. Reflections into Ptolemaic glass: colorless, white, blue, and green inlays from the workshop of Tebtynis. *Archaeometry* **65**, 653–690 (2023).
- Bettineschi, C. & Angelini, I. Reflections into Ptolemaic glass II: characterizing yellow, yellowish-orange, red, and brown inlays from tebtynis. *Archaeometry* **66**, 119–141 (2024).
- Boschetti, C. Working glass in Ptolemaic Egypt, new evidence from Denderah. *J. Archaeol. Sci. Rep.* **22**, 550–558 (2018).
- Sayre, E. V. The intentional use of antimony and manganese in ancient glasses in *Advances in Glass Technology, Part 2* (eds. Matson, F. R. & Rindone, G. E.) 263–282 (New York, 1963).
- Reade, W. *The First Thousand Years of Glass-Making in the Ancient Near East: Compositional Analyses of Late Bronze and Iron Age Glasses* (Oxford, 2021).
- Brill, R. H. Laboratory studies of some glasses from Vergina. *J. Glass Studies*, pp. 11–23 (JSTOR, 1994).
- Henderson, J. *Ancient Glass: An Interdisciplinary Exploration* (Cambridge, 2013).
- Lichtenberger, A. et al. For everything there is a season: more than a year of destruction at Seleucid Tell Izṭabba (Israel). *Antiquity* **96**, 1316–1323 (2022).
- Edrey, M., Ebeling, P., Harpak, T., Lichtenberger, A. & Tal, O. Field report on the 2023 German-Israeli Tell Izṭabbā Excavation Project (Beth She'an), Israel. *Zeitschrift des Deutschen Palästina-Vereins* **139** (2023).
- Lichtenberger, A. & Tal, O. Hellenistic Nysa-Scythopolis I: The German-Israeli Tell Izṭabba Excavation Project. The 2019–2020 Seasons (Tel Aviv University Monograph Series of the Institute of Archaeology 44) (University Park & Tel Aviv, 2025).
- Jackson-Tal, R. E. Vitreous finds: faience and glass in Hellenistic Nysa-Scythopolis I: The German-Israeli Tell Izṭabba Excavation Project. The 2019–2020 Seasons (eds. Lichtenberger, A. & Tal, O.) 165–182 (Tel Aviv University Monograph Series of the Institute of Archaeology 44, University Park & Tel Aviv, 2025).
- Paton, C., Hellstrom, J., Paul, B., Woodhead, J. & Hergt, J. Lolite: Freeware for the visualisation and processing of mass spectrometric data. *J. Anal. At. Spectrom.* **26**, 2508–2518 (2011).
- Woodhead, J., Hellstrom, J., Hergt, J., Greig, A. & Maas, R. Isotopic and elemental imaging of geological materials by laser ablation inductively coupled plasma-mass spectrometry. *Geostand. Geoanal. Res.* **31**, 331–343 (2007).
- Barfod, G. H., Freestone, I. C., Leshner, C. E., Lichtenberger, A. & Raja, R. Alexandrian glass confirmed by hafnium isotopes. *Sci. Rep.* **10**, 11322 (2020).
- Bouvier, A., Vervoort, J. D. & Patchett, P. J. The Lu–Hf and Sm–Nd isotopic composition of CHUR: constraints from unequilibrated

- chondrites and implications for the bulk composition of terrestrial planets. *Earth Planet Sci. Lett.* **273**, 48–57 (2008).
23. Price, J., Freestone, I. C. & Cartwright, C. R. C. ‘All in a day’s work?’ The colourless cylindrical glass cups found at Stonea revisited in Image, Craft and the Classical World: Essays in Honour of Donald Bailey and Catherine Johns (ed. Crummy, N.) 163–169 (Collection ‘Monographies Instrumentum’ 29) (Montagnac, 2005).
  24. Freestone, I. C., Price, J. & Cartwright, C. The batch: its recognition and significance. *Actes du Colloque de l’Association Française pour l’Archéologie du Verre* **17**, 130–135 (2009).
  25. Freestone, I. C., Jackson-Tal, R., Tal, O. & Taxel, I. Glass production at an Early Islamic workshop in Tel Aviv. *J. Arch. Sci.* **62**, 45–54 (2015).
  26. Barfod, G. H., Freestone, I. C., Jackson-Tal, R. E., Lichtenberger, A. & Raja, R. Exotic glass types and the intensity of recycling in the northwest Quarter of Gerasa (Jerash, Jordan). *J. Archaeol. Sci.* **140**, 105546 (2022).
  27. Freestone, I. C., Barfod, G. H., Chen, C., Larson, K. A. & Gorin-Rosen, Y. Glass production at Jalame, Israel: process, composition and relationship to Roman glass in Europe. *J. Arch. Sci. Rep.* **51**, 104179 (2023).
  28. Paynter, S. & Jackson, C. Clarity and brilliance: antimony in colourless natron glass explored using Roman glass found in Britain. *Archaeol. Anthropol. Sci.* **11**, 1533–1551 (2019).
  29. Ganio, M. et al. Trade routes across the Mediterranean: A Sr/Nd isotopic investigation on Roman colourless glass. *Glass Technol. -Eur. J. Glass Sci. Technol. Part A* **53**, 217–224 (2012).
  30. Gallo, F. et al. Roman and Late-Roman glass from north-eastern Italy: the isotopic perspective to provenance its raw materials. *J. Arch. Sci.* **62**, 55–65 (2015).
  31. Lü, Q. Q., Henderson, J., Wang, Y. & Wang, B. Natron glass beads reveal proto-Silk Road between the Mediterranean and China in the 1st millennium BCE. *Sci. Rep.* **11**, 3537 (2021).
  32. Freestone, I. C., Leslie, K. A., Thirlwall, M. & Gorin-Rosen, Y. Strontium isotopes in the investigation of early glass production: Byzantine and Early Islamic glass from the Near East. *Archaeometry* **45**, 19–32 (2003).
  33. Ganio, M. et al. Roman glass across the Empire: an elemental and isotopic characterization. *Anal. Atom. Spectrom.* **27**, 743–753 (2012).
  34. Veizer, J. et al.  $^{87}\text{Sr}/^{86}\text{Sr}$ ,  $\delta^{13}\text{C}$  and  $\delta^{18}\text{O}$  evolution of Phanerozoic seawater. *Chem. Geol.* **161**, 59–88 (1999).
  35. Degryse, P. & Schneider, J. Pliny the Elder and Sr–Nd isotopes: tracing the provenance of raw materials for Roman glass production. *J. Archaeol. Sci.* **35**, 1993–2000 (2008).
  36. Vervoort, J. D. & Blichert-Toft, J. Evolution of the depleted mantle: Hf isotope evidence from juvenile rocks through time. *Geochim. Cosmochim. Acta.* **63**, 533–556 (1999).
  37. Foy, D., Picon, M., Vichy, M. & Thirion-Merle, V. Caractérisation des verres de la fin de l’Antiquité en Méditerranée occidentale: L’émergence de nouveaux courants commerciaux in Echanges et commerce du verre dans le monde antique: actes du colloque de l’Association Française pour l’antiquité du Verre, Aix-en-Provence et Marseille, 7–9 Juin 2001 (eds. Foy, D. & Nenna, M.-D.) 41–86 (Montagnac, 2003).
  38. Freestone, I. C., Brems, D. & Degryse, P. Composition of late Hellenistic to early Roman glass vessels from the Souk Excavations, Beirut. *Rend. Lincei. Sci. Fis. Nat.* **36**, 39–48 (2025).
  39. Schibille, N., Sterrett-Krause, A. & Freestone, I. C. Glass groups, glass supply and recycling in late Roman Carthage. *Archaeol. Anthropol. Sci.* **9**, 1223–1241 (2017).
  40. Silvestri, A., Molin, G. & Salviulo, G. The colourless glass of Iulia Felix. *J. Archaeol. Sci.* **32**, 331–341 (2008).
  41. Freestone, I. C., Gorin-Rosen, Y. & Hughes, M. J. Composition of primary glass from Israel in La route du verre: ateliers primaires et secondaires de verriers du second millénaire av. J.-C. au Moyen-Âge (ed. Nenna, M.-D.) 65–84 (Travaux de la Maison de l’Orient Méditerranéen 33) (Lyon, 2000).
  42. Tal, O., Jackson-Tal, R. E. & Freestone, I. C. New evidence of the production of raw glass at Late Byzantine Apollonia-Arsuf (Israel). *J. Glass Stu* **46**, 51–66 (2004).
  43. Phelps, M., Freestone, I. C., Gorin-Rosen, Y. & Gratuze, B. Natron glass production and supply in the late antique and early medieval Near East: The effect of the Byzantine-Islamic transition. *J. Arch. Sci.* **75**, 57–71 (2016).
  44. Trowbridge, M. L. *Philological Studies In Ancient Glass* (Urbana-Champaign, 1930).
  45. Kouwatli, I. et al. A pottery and glass production site in Beirut (BEY 015). *BAAL* **10**, 103–130 (2008).
  46. Goldsmith, S. L., Krom, M. D., Sandler, A. & Herut, B. Spatial trends in the chemical composition of sediments on the continental shelf and slope off the Mediterranean coast of Israel. *Cont. Shelf Res.* **21**, 1879–1900 (2001).
  47. Oikonomou, A., Henderson, J., Gnade, M., Chenery, S. & Zacharias, N. An archaeometric study of Hellenistic glass vessels: evidence for multiple sources. *Archaeol. Anthropol. Sci.* **10**, 97–110 (2018).
  48. Reade, W. J. & Privat, K. L. Chemical characterisation of archaeological glasses from the Hellenistic site of Jebel Khalid, Syria by electron probe microanalysis. *Herit. Sci.* **4**, 20 (2016).
  49. Schreurs, J. W. & Brill, R. H. Iron and sulfur related colors in ancient glasses. *Archaeometry* **26**, 199–209 (1984).
  50. Jackson, C. M. & Paynter, S. A. Great big melting pot: exploring patterns of glass supply, consumption and recycling in Roman Coppergate, York. *Archaeometry* **58**, 68–95 (2016).
  51. Silvestri, A. The coloured glass of Iulia Felix. *J. Archaeol. Sci.* **35**, 1489–1501 (2008).
  52. Degryse, P. *Glass Making in the Greco-Roman World: Results of the ARCHGLASS Project.* (Leuven University Press, 2014).
  53. Freestone, I. C. Re-use and recycling of roman glass: analytical approaches. *J. Glass Stud.* **57**, 29–40 (2015).
  54. Gliozzo, E. The composition of colourless glass: a review. *Archaeol. Anthropol. Sci.* **9**, 455–483 (2017).
  55. Boschetti, C. et al. Glass working and recycling in Pompeii: new evidence from the landfill of the Sarno Baths (VIII 2, 17–23). *Archaeol. Anthropol. Sci.* **16**, 115 (2024).
  56. Erim, K. T. & Reynolds, J. The aphrodisias copy of diocletian’s edict on maximum prices. *J. Rom. Stud.* **63**, 99–110 (1973).
  57. Stern, E. M. Ancient glass in philological context. *Mnemosyne* **60**, 341–406 (2007).
  58. Balvanović, R. V. & Šmit, Ž. Emerging glass industry patterns in late antiquity balkans and beyond: new analytical findings on Foy 3.2 and Foy 2.1 glass types. *Materials* **15**, 1086 (2022).

## Acknowledgements

The work was supported by the Deutsche Forschungsgemeinschaft (DFG) – Research Grant (Projektnummer 495961685) – Tell Iztabba (Nysa-Skythopolis) – eine seleukidische Gründung im Nahen Osten, 2022–2025, awarded to AL and OT. The authors thank P.L. Baker (GeoAnalytical Lab, WSU) for performing isotope analysis.

## Author contributions

G.B.: Writing – original draft, Methodology, Investigation, Formal analysis. I.F.: Writing – original draft, Methodology, Investigation, Formal analysis. R.J.-T.: Writing – original draft, Conceptualisation, Investigation, Data curation. A.C.-U.: LA-ICPMS, Data curation. A.L.: Writing – original draft, Conceptualisation, Investigation, Funding acquisition, Data curation. O.T.: Writing – original draft, Conceptualisation, Investigation, Funding acquisition, Data curation.

## Funding

Open Access funding enabled and organized by Projekt DEAL.

### Competing interests

The authors declare no competing interests.

### Additional information

**Supplementary information** The online version contains supplementary material available at

<https://doi.org/10.1038/s40494-025-02139-2>.

**Correspondence** and requests for materials should be addressed to Achim Lichtenberger.

**Reprints and permissions information** is available at <http://www.nature.com/reprints>

**Publisher's note** Springer Nature remains neutral with regard to jurisdictional claims in published maps and institutional affiliations.

**Open Access** This article is licensed under a Creative Commons Attribution 4.0 International License, which permits use, sharing, adaptation, distribution and reproduction in any medium or format, as long as you give appropriate credit to the original author(s) and the source, provide a link to the Creative Commons licence, and indicate if changes were made. The images or other third party material in this article are included in the article's Creative Commons licence, unless indicated otherwise in a credit line to the material. If material is not included in the article's Creative Commons licence and your intended use is not permitted by statutory regulation or exceeds the permitted use, you will need to obtain permission directly from the copyright holder. To view a copy of this licence, visit <http://creativecommons.org/licenses/by/4.0/>.

© The Author(s) 2025